Energy Conversion and Management: X 30 (2026) 101667

Contents lists available at ScienceDirect

Energy Conversion and Management: X

journal homepage: www.sciencedirect.com/journal/energy-conversion-and-management-x

Techno-economic analysis of High-Temperature Aquifer Thermal Energy Storage in district heating systems

David Geerts [a,*], Wen Liu [a], Alexandros Daniilidis [b], Philip J. Vardon [b], Gert Jan Kramer [a]

[a] Copernicus Institute of Sustainable Development, Heidelberglaan 8, 3584 CS, Utrecht, The Netherlands
[b] Faculty of Civil Engineering and Geosciences, Delft University of Technology, Stevinweg 1, 2628 CN, Delft, The Netherlands

ARTICLE INFO

Keywords:
High-Temperature Aquifer Thermal Energy Storage
District heating
Levelized cost of heat
Carbon abatement cost
Monte Carlo
Peak shaving

ABSTRACT

Integrating renewable energy into district heating creates a heat supply–demand mismatch that High-Temperature Aquifer Thermal Energy Storage (HT-ATES) can help address. However, the potential greenhouse gas emission reduction and financial benefits of HT-ATES have received limited attention. Additionally, the interplay between the demand, supply components, and HT-ATES has been overlooked, while the assessment of integrating HT-ATES into a district heating system is crucial to understanding the benefits of the HT-ATES implementation. This study evaluates the integration of HT-ATES into a district heating system, focusing on both economic and environmental performance indicators. It novelly accounts for the dynamic operational interactions between HT-ATES and other system components, enabling a more realistic assessment of operational choices. The model is applied to a case study of a simplified district heating system. The results show that the relative size of the heat supplier compared to heat demand is a key determinant of the cost-effectiveness of HT-ATES. In the case study, a geothermal doublet reduced the levelized cost of heat by 25–37 €/MWh compared to a gas boiler, while also reducing reliance on fossil fuels. In contrast, HT-ATES had a limited impact on total system costs, regardless of whether it operated when stored heat was available or was used for peak shaving. Nevertheless, HT-ATES increased the renewable energy share by 9%–18% across all scenarios. Furthermore, the optimal geothermal capacity differed depending on whether HT-ATES was included. Finally, while a high renewable energy share can be cost-effective, achieving 100% renewable heat was found to be highly cost-ineffective in this case. These results support informed decision-making on HT-ATES implementation under appropriate system design conditions.

1. Introduction

Mitigating greenhouse gas emissions is one of the greatest challenges of the 21st century. Heating and cooling systems account for around 65% of global energy consumption in buildings [1], the majority of which is covered by fossil fuels [2]. Transitioning to sustainable heat sources is complex due to discrepancies between supply and demand profiles [3]. For example, geothermal energy provides constant heat year-round at low operational costs [4], while solar heat fluctuates daily and seasonally [5]. Heat demand, however, peaks in colder seasons and drops in warmer ones. Seasonal Thermal Energy Storage (STES) is a key technology to address this challenge.

STES enables long-term heat storage, typically over months, to address seasonal supply–demand mismatches. One such technology, Aquifer Thermal Energy Storage (ATES), stores excess heat in an underground aquifer and retrieves it when needed, reducing greenhouse gas emissions when replacing fossil-fuelled backup sources. Most ATES systems operate at temperatures below 25 °C [6], which is insufficient for District Heating (DH) systems that require higher operating temperatures.

HT-ATES, operating at temperatures ≥25 °C, can be more efficient to use compared to low-temperature ATES systems, as they can provide heat directly to the demand. This allows HT-ATES to balance supply and demand by using excess heat. The HT-ATES can also reduce the need for large backup capacity by providing peak shaving, making it a potentially cost-effective option for DH systems.

A recent review [7] highlights that the cost-effectiveness and environmental benefits of HT-ATES are under explored. Some studies have focused on these aspects for ATES operating below <25 °C [8–10], while for HT-ATES these studies are sparse despite the importance of these factors [11]. While more recently a study showed the lessons learned from different HT-ATES projects, showing the importance of the economic performance [12], another recent study published a play-based assessment of the feasibility of HT-ATES [13]. To the authors'

* Corresponding author.
E-mail address: d.c.geerts@uu.nl (D. Geerts).

https://doi.org/10.1016/j.ecmx.2026.101667
Received 24 June 2025; Received in revised form 6 February 2026; Accepted 9 February 2026
Available online 10 February 2026

Abbreviations

$\frac{G}{D}$	Ratio of Geothermal to Demand
CAC	Carbon Abatement Cost
DH	District Heating
G	Gas-only configuration
GG	Gas + geothermal configuration
GGA	Gas + geothermal + HT-ATES configuration
HT-ATES	High-Temperature Aquifer Thermal Energy Storage
LCOH	Levelized Cost Of Heat
RES	Renewable Energy Share
STES	Seasonal Thermal Energy Storage

knowledge, only three studies addressed HT-ATES's economic and environmental impacts [14,15]. Daniilidis et al. [14] primarily focused on the impacts of subsurface parameters on the performance of the HT-ATES. They identified aquifer transmissivity as the key factor influencing the LCOH of a HT-ATES. Bloemendal et al. [15] examined one case study with four business cases; they elaborated on the technical, economic, and environmental assessment of the HT-ATES on the case study. However, these studies do not consider the dynamic operational interplay between HT-ATES and other DH system components, such as heat demand profiles, heat supply capacities, charging and discharging strategies, and operating temperatures. This lack of a system-level perspective represents a significant knowledge gap. The interaction between HT-ATES and DH components directly affects storage utilization, peak demand coverage, operational temperatures, and ultimately the economic and environmental performance of the entire DH system.

Furthermore, HT-ATES is often mentioned as a peak shaving technology in a DH system [16,17], however, no study has yet quantified the economic benefit of this potential function. Quantifying these benefits would provide insight into the benefits that HT-ATES can serve in a DH system.

This study addresses these gaps by developing a system-level modelling framework to assess the technical, economic, and environmental performance of HT-ATES integrated into a DH system. The model explicitly captures the operational interplay between HT-ATES and other DH components and quantifies key performance indicators, including LCOH, renewable energy share (RES), and carbon abatement cost (CAC). The framework is applied to a case study based on a simplified DH system inspired by Delft University of Technology in the Netherlands. Multiple system configurations are evaluated to assess the influence of HT-ATES size, heat supply capacity, and cut-off temperature. In addition, the economic benefits of peak shaving are quantified, and a Monte Carlo analysis is conducted to assess uncertainty in LCOH.

2. Modelling approach

A DH system is designed to fulfil a certain heat demand, with one or more heat suppliers and possibly a HT-ATES. These components (supply, demand, and storage) are interconnected via DH infrastructure.

The basis for the modelling is that the heat demand always needs to be met. This demand is represented by an hourly heat load, with a predefined supply and return temperature (also called cut-off temperature). The DH network is not explicitly modelled, excluding modelling the heat exchangers, pumps, valves, and daily buffers required for operating a DH system. However, its installation and operation costs are included in the economic assessment, which is explained below. A schematic representation of the system can be found in Fig. 1(a)

2.1. Control strategy

Heat demand is met using a general control system that activates at each time step, following this merit order:

1. Sustainable heat supply technologies are activated, which often have a lower operational cost compared to fossil fuel-based ones.
2. The HT-ATES is activated.
    2.1. If heat supply exceeds demand, excess heat is stored up to a predefined maximum; any surplus is curtailed.
    2.2. If demand exceeds supply, stored heat is extracted.
3. Any remaining unmet demand is covered by backup sources.

This process, visualized in Fig. 1(b), operates on hourly time steps and accommodates various DH components. For the model application in this study, the system includes deep geothermal, HT-ATES, and a gas boiler. The modelling of these components is detailed in the following sections.

2.2. Model components

2.2.1. Deep geothermal heat

Deep geothermal heat extraction provides a base load source, providing a constant heat supply year-round with a fixed flow rate and temperature. The generated heat is calculated using:

$$E = mc\Delta T. \tag{1}$$

E is the heat delivered (J), m is the mass (kg), c is the specific heat capacity (J/(kg°C)), and the used fluid is assumed to be water. ΔT is the temperature difference (°C) between the geothermal output and the cut-off temperature.

2.2.2. HT-ATES

The HT-ATES model, developed by Geerts et al. [18], requires two operational parameters: total yearly injected volume and injected temperature. Additionally, it requires aquifer parameters, including porosity, aquifer thickness, horizontal hydraulic conductivity, anisotropy, and undisturbed ground temperature [18]. The model outputs the temperature profile and flow rate, determining the extractable energy. In this model, a machine learning algorithm is applied to calculate the recovery efficiency of the HT-ATES. Using this recovery efficiency and two other parameters, the most suitable temperature profile is extracted from a large dataset. This temperature profile is used to estimate the efficiency of the HT-ATES. This HT-ATES is constrained by a maximum pumping rate, assumed equal for injection and extraction, which limits the amount of heat stored or extracted at each time step. The model was shown to be accurate, with a root mean square error in efficiency prediction of 1.4 percentage points [18], with a lower accuracy in low efficiency systems.

2.2.3. Gas boiler

The gas boiler meets all remaining unmet demand, burning natural gas at an assumed efficiency of 93% [19]. The capacity of the gas boiler is scaled to provide 110% of its maximum load, ensuring that there is always enough capacity to meet the peak demand.

3. Assessment metrics

Techno-economic and environmental assessments evaluate the costs and benefits of each component and the DH system when adding HT-ATES.

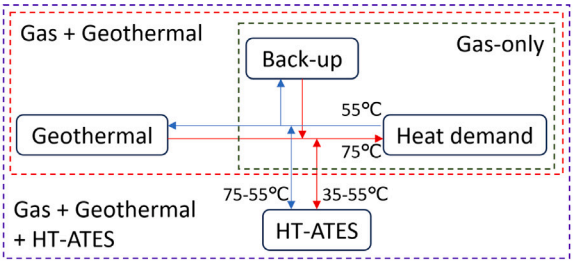

(a) Schematic representation of the used DH system and the connections between components, red indicating hot flows, blue indicating cold flows. The different configurations used are also displayed (see Section 4.2)

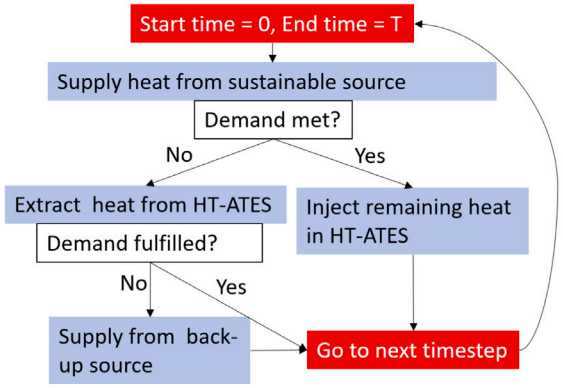

(b) Control system for modelling the DH system.

Fig. 1. Schematic overview and control system of the DH system.

3.1. Economic assessment

The economic assessment metric is LCOH. This metric allows for a comparison between different heat technologies. Both the system LCOH and the LCOH of individual components are calculated. The LCOH of individual components is used to compare the components with each other, while the system LCOH is used to compare different heating systems' costs. This calculation is based on Yang et al. [7], and it is defined as

$$LCOH = \frac{\sum_{t=1}^{n} \frac{I_t + O\&M_t}{(1+r)^t}}{\sum_{t=1}^{n} \frac{E_t}{(1+r)^t}}. \quad (2)$$

where I_t is the investment to install the component (€), r is the discount rate, n is the lifetime (years), $O\&M$ is the annual cost of operation and maintenance (€), and E_t is the annual heat delivered to the demand (kWh). The heat supplied from deep geothermal to HT-ATES is excluded from the geothermal E_t, and the additional costs (OpEx) for generating this heat are reassigned to HT-ATES. For the LCOH of the system, the same formula is used. However, in E_t, the excess energy stored in the storage is not included as it is not delivered to the demand [7]. The lifetime of the system is chosen as the smallest value that ensures no residual value at the end of the system's life. Components are replaced as needed, with replacement costs included in the relevant year's O&M.

3.2. Environmental assessment

The used metrics in the environmental assessment are the Carbon Abatement Cost (CAC) and Renewable Energy Share (RES). The CAC measures the cost in euros to reduce one kg CO_2 emission, comparing a system with and without a specific component. It is calculated as follows [20]

$$CAC = \frac{LCOH_{system1}}{EF_{system1}} - \frac{LCOH_{system2}}{EF_{system2}}, \quad (3)$$

where $LCOH_{system1}$ and $LCOH_{system2}$ are the LCOH for the system with and without the component, respectively. EF is the emission factor, calculated as

$$EF = \frac{\sum_{t=1}^{n} \frac{CO_{2,s,t}}{(1+r)^t}}{\sum_{t=1}^{n} \frac{E_{s,t}}{(1+r)^t}}. \quad (4)$$

$CO_{2,s,t}$ is the total CO_2 emissions of the system in year t (kg CO_2), calculated by summing the CO_2 of the individual components, only taking into account the emissions created during the operation of the system. For the HT-ATES, CO_2 emissions are calculated based on the CO_2 emissions of the source supplying the HT-ATES and the emissions of operating the HT-ATES itself. The emissions related to the stored heat are subtracted from the deep geothermal and added to the HT-ATES.

The RES is also calculated, representing the share of energy that is supplied by renewable sources relative to the total energy delivered. It is calculated as follows [7]

$$RES = E_{RES}/E_{tot}, \quad (5)$$

where E_{RES} is the energy delivered by renewable sources (kWh) and E_{tot} is the total energy delivered (kWh).

4. Case study

The model is applied to a case study of a simplified DH system conceptually based on Delft, the Netherlands, using a feasibility study for the TU Delft campus and surrounding areas [15]. The focus of the case study is on the heat generation and demand, therefore, the hydraulics of a DH system are neglected. Furthermore, the actual DH system in Delft is going to be using a heat pump, and the used economic parameters are more generic than the actual values for the Delft DH. The case shows the model application with one representative sustainable heat supply technology rather than the application to a specific DH system.

4.1. Case description

The DH of the case study is currently supplied by gas boilers. A deep geothermal doublet and a HT-ATES are developed to supply heat to the DH system [15].

4.1.1. Technical details

The supply temperature of the DH system is fixed in the model to 75 °C with a return temperature of 55 °C [15]. Multiple demand curves were used, as explained below. The geothermal doublet delivers 320 m^3/h of 75 °C, delivering 7.4 MW of heat. The HT-ATES is scaled to inject and extract 320 m^3/h. The aquifer has a thickness of 55 m, a horizontal hydraulic conductivity of 10 m/d, a vertical hydraulic conductivity of 2 m/d, a ground temperature of 15 °C and a porosity of 0.3 [15]. The gas boilers are sized to deliver the unmet demand, and they are assumed to be newly installed for the calculation of the LCOH to allow a fair comparison between technologies.

Table 1
Economic and environmental parameters used in the case study.

Component	Parameter	Value	Unit	Source
Geothermal	Capex	1.91	M€/MW	[23]
	Fixed opex	69	k€/MW per year	[23]
	Variable opex	7.2	€/MWh per year	[23]
	Lifetime	30	years	[23]
	CO_2 emissions	12.5	$kgCO_2$/MWh	[21]
Gas boiler	Capex	0.1	M€/MW	[24]
	Fixed opex	2	k€/MW	[24]
	Gas price (including tax)	55	€/MWh	[25]
	Lifetime	15	years	[26]
	CO_2 emissions	200	$kgCO_2$/MWh	[27]
HT-ATES	Capex	0.01	M€/(m^3/h injection capacity)	[15]
	Fixed opex	0.77	k€/(m^3/h injection capacity)/year	[15]
	Electricity use	1.39	kWh/m^3 injected	[15]
	Electricity price	200	€/MWh	[28]
	Lifetime	30	years	[24,29]
	CO_2 emissions electricity	0	$kgCO_2$/MWh	[21]
System	Discount rate	5	%	[7]
	Network CapEx	1157	€/m	[15,30]
	Network OpEx	2	% of CapEx per year	[30,31]
	Lifetime	60	years	[32]

4.1.2. Economic and environmental inputs

The economic and environmental details of the components can be found in Table 1. The total OpEx is calculated by multiplying the fixed OpEx by the capacity of the component and the variable OpEx by the heat generated by the component. For the gas boiler, this variable OpEx is the gas price; for the HT-ATES, the variable OpEx is the multiplication of electricity use, electricity price, and yearly injected and extracted volume. The HT-ATES CO_2 emissions are zero, as the electricity is assumed to be renewable [21]. There is also a price for the CO_2 emissions, in line with the 2030 Dutch CO_2 tax, which is 150 euros/tonne CO_2 [22]. The DH system costs are found under the system component, and the lifetime under that same component reflects the lifetime of the DH system.

4.2. Configurations comparison

Three demand cases are used to analyse the HT-ATES interaction with the DH system, based on the TU Delft campus and the new DH system for Delft city [15]. They are named after their level of demand compared to the supply from the geothermal doublet. For this, the $\frac{G}{D}$ is introduced, which is defined as the total available geothermal heat production divided by the total heat demand. The $\frac{G}{D}$ is calculated using the 7.4 MW geothermal doublet, as discussed in Section 4.1.1. The following cases are used: (1) TU Delft (called $\frac{G}{D}$ = 1.62); (2) Delft City ($\frac{G}{D}$ = 1.07); (3) Delft Total (TU + Delft City) ($\frac{G}{D}$= 0.65), where the third case is the sum of the first and second cases. The demand curves of $\frac{G}{D}$ = 1.62 and 1.07 are shown in Fig. 2. The demand is assumed to be the same for the entire lifetime of the system. The network length is 8 km and 15 km for $\frac{G}{D}$= 1.62 and $\frac{G}{D}$ = 1.07, respectively.

The three configurations represent different supply technologies being used and are as follows: (1) Gas only (Abbreviated as G); (2) Gas + Geothermal (GG); (3) Gas + Geothermal + HT-ATES (GGA). These configurations can be seen in Fig. 1(a). All three demand cases are combined with all three configurations, leading to 9 combinations. For all, the LCOH, CAC, and RES are calculated and compared.

4.3. Parameter exploration

To further analyse the case study and increase the knowledge on interaction between DH system components, the effect of several key parameters is tested with a one-at-a-time (OAT) sensitivity analysis. The resulting LCOH and RES are compared. The tested parameters are:

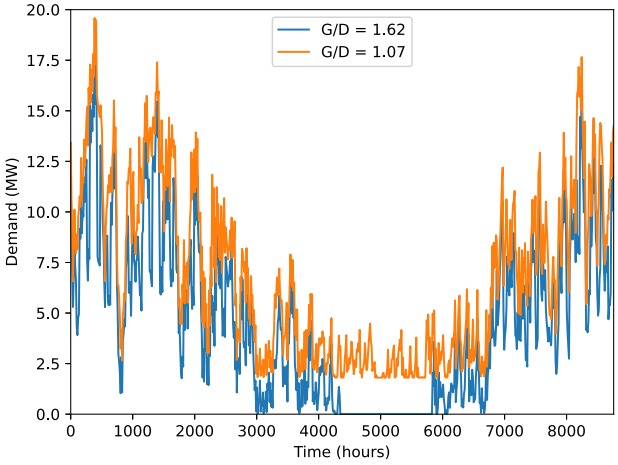

Fig. 2. Demand data of $\frac{G}{D}$ = 1.62 and 1.07. Obtained from [15]. The average yearly demand is 4.5 MW and 6.9 MW for $\frac{G}{D}$ = 1.62 and 1.07, respectively.

- Geothermal doublet capacity, which is likely to be important for the LCOH of the system. This is implemented by modifying the geothermal doublet extraction rate relative to the average demand. This reflects the seasonality of the demand, and this $\frac{G}{D}$ is varied between 0.25 and 3 by changing the geothermal flow rate and, therefore, the geothermal capacity. The heat demand is kept the same.
- HT-ATES maximum pumping rate, which determines the rate of heat that can be stored and extracted, which influences both the efficiency of the HT-ATES system and the maximum heat extraction at each single time step [33]. This shows the impact of size on the HT-ATES LCOH. The size is varied between 30 and 350 m^3/h.
- Cut-off temperature, which determines the amount of useful heat from the HT-ATES and geothermal doublet and, therefore, is an important parameter to test. It varies between 45 °C and 65 °C. No additional costs were incurred to do so.

4.4. HT-ATES operation approach

This subsection outlines the methodology used to evaluate the effects of peak shaving, as well as highlighting LCOH changes by using a different calculation approach. Two tests were designed to do so.

Table 2
Monte Carlo probability distributions for the economic parameters. s.d. is the standard deviation that was used for the probability distribution.

Parameter	Distribution	Value	Unit	Source
Gas price	Normal	Mean: 55, s.d.:5	€/MWh	[35]
Electricity price	Normal	Mean: 200, s.d.:30	€/MWh	[28,36]
CO2 price	Normal	Mean: 150, s.d.:5	€/tonne CO_2	[22]
CapEx gas	Normal	Mean: 0.1, s.d.:0.005	€/MW	
CapEx HT-ATES	Normal	Mean: 0.01, s.d.:0.003	M€/(m^3 injection rate)	
CapEx Geo	Normal	Mean: 1.909, .d.:0.3	€/MW	

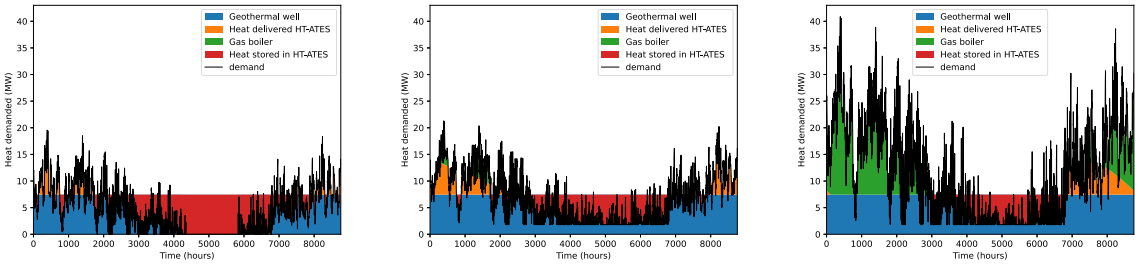

(a) Demand profile $\frac{G}{D}$ = 1.62, average yearly demand = 4.5 MW and the largest peak is 19.6 MW

(b) Demand profile $\frac{G}{D}$ = 1.07, average yearly demand = 6.9 MW and the largest peak is 21.3 MW

(c) Demand profile $\frac{G}{D}$ = 0.65, average yearly demand = 11.4 MW and the largest peak is 40.8 MW

Fig. 3. Heat supplied to the demand by source.

The first test is that a HT-ATES system is less efficient during the first few years of operation, as the subsurface needs to be warmed up [34]. This effect is often not mentioned and neglected in economic analysis of HT-ATES, but it is implemented in the HT-ATES model used in this study.

The LCOH of the HT-ATES is evaluated using two different approaches: The first assumes a constant recovery efficiency throughout the HT-ATES's lifetime, which is equal to the recovery efficiency calculated by the HT-ATES model after 8 years [18]. The second approach accounts for the lower recovery efficiency during the initial years. This lower efficiency is obtained using the HT-ATES model [18]. By comparing these two methods, the impact of neglecting the inefficiency of the first few years on the LCOH can be assessed.

The second test is on the technical function of "peak shaving", mentioned in the literature [16,17]. It means HT-ATES can reduce the most prominent peak of the demand and, therefore, requires smaller backup equipment, in this case, gas boilers [16,17]. The economic benefits of peak shaving served by HT-ATES are quantified in this study by modifying the control system described in Section 2.1. Instead of extracting from the storage when possible, the control is changed so that the HT-ATES extraction is proportional to the unmet demand. Therefore, the extraction of the HT-ATES is large when the unmet demand is large and small when the unmet demand is small. Previously, the control system ensured that the HT-ATES extraction was as soon as possible. This new approach quantifies the savings that are created by having smaller backup equipment.

4.5. Monte Carlo analysis

Lastly, a Monte Carlo is applied to assess the impact of uncertainty in the economic parameters. This shows the uncertainty of the system LCOH and generates a range of the system LCOH. With 20,000 iterations using randomly generated inputs based on predefined probability distributions, the simulation provides a range for the system LCOH. This number of iterations results in the P10 and P90 values differing by less than 1% when doing multiple different runs of 20,000 iterations, signifying a converged result. The LCOH distribution was calculated for each demand case and only for the Gas + Geothermal + HT-ATES configuration. The economic parameters and their probability distribution are shown in Table 2.

5. Results

5.1. Heat supply and LCOH

The demand profiles for the three demand cases are shown in Fig. 3. For the $\frac{G}{D}$ = 1.62 case, the deep geothermal source supplies 86% of the required heat (Fig. 3(a)). Consequently, a substantial amount of heat is stored in the HT-ATES, which has an efficiency of 86.6% in this case [18], covering much of the peak demand. Over 99% of the energy is provided by the geothermal doublet and HT-ATES, with minimal supplementary heating from gas boilers. For the $\frac{G}{D}$ = 1.07 case, more geothermal heat is directly delivered to the demand compared to the $\frac{G}{D}$ = 1.62 case (Fig. 3(b)), which is due to the increased heat demand during the summer in $\frac{G}{D}$ = 1.07. Lastly, for the $\frac{G}{D}$ = 0.65 case (Fig. 3(c)), most of the geothermal heat is directly used, resulting in less excess heat being stored in the HT-ATES, compared to the other two cases. This decreases the efficiency of the HT-ATES a little to 83.9%. Consequently, the HT-ATES provides very little heat during the cold season.

The LCOH of each component and the system can be found in Fig. 4. The LCOH of a gas-only system remains consistent around 94 €/MWh. The difference between the LCOH of the system and the gas component is caused by the costs of the DH systems infrastructure.

When geothermal energy is introduced (gas + geothermal), the system LCOH decreases between 25 and 37 €/MWh for all demand cases compared to the gas-only system due to the geothermal doublet's cost-effectiveness. The difference of geothermal LCOH between different demand cases is due to the amount of heat that can be directly provided to the demand from geothermal energy. As seen in Fig. 3, geothermal energy supplies the most in the $\frac{G}{D}$ = 0.65 case, and the least in the $\frac{G}{D}$ = 1.62 case, which is reflected in the LCOH of geothermal. The LCOH of the gas boiler increases slightly for each demand case compared to the gas-only. With geothermal energy added, the load of the gas boiler is lower relative to its capacity compared to gas-only, which increases its LCOH (see Fig. 5(a) for RES and gas boiler share). This effect is least noticeable in the $\frac{G}{D}$ = 0.65 demand because a large share of the heat is still provided by the gas boiler, leading to a high load and a lower LCOH of the gas boiler (Fig. 3(c)).

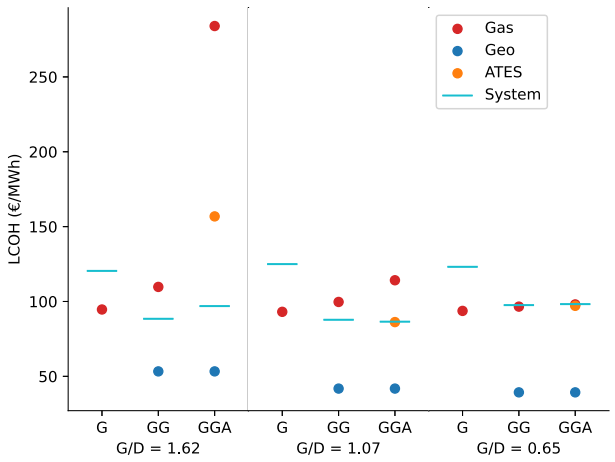

Fig. 4. LCOH of the nine combinations, G is gas-only, GG is gas + geothermal, GGA is gas + geothermal + HT-ATES.

In the gas + geothermal + HT-ATES configuration the LCOH of the HT-ATES system is 157 €/MWh, 86 €/MWh, and 97 €/MWh for the cases $\frac{G}{D}$ = 1.62, 1.07, and 0.65, respectively. For context, the price ceiling for heat in the Netherlands for DH systems is 158 €/MWh [37]. The system LCOH decreases only in the $\frac{G}{D}$ = 1.07 case compared to the GG configuration, while for the other demand cases, the system LCOH increases, showing that the HT-ATES is not always economically beneficial. The geothermal LCOH remains constant between configurations since all additional heat produced and additional cost incurred due to this produced heat are attributed to the HT-ATES. For $\frac{G}{D}$ = 1.62 and 1.07, the LCOH of the gas boiler is also relatively large due to the large capacity relative to the amount of heat it provides. The HT-ATES is most cost-effective with the $\frac{G}{D}$ = 1.07 case because a large amount of heat is both stored and retrieved from the HT-ATES. The other two cases are less cost-effective. For the $\frac{G}{D}$ = 1.62, the injected heat is much larger than the extracted heat, leading to underutilization of the HT-ATES capacity. For the $\frac{G}{D}$ = 0.65 demand, the amount of injected heat is smaller than the $\frac{G}{D}$ = 1.07, and therefore, the amount of extracted heat is smaller as well, while the investment cost remains the same between all demand cases.

In conclusion, the geothermal doublet is highly cost-efficient, with the HT-ATES being beneficial in the $\frac{G}{D}$ = 1.07 case. The lowest system LCOH is found in this case with the GGA configuration at 87 €/MWh, significantly below the Dutch price cap of 158 €/MWh [37].

5.2. RES and CAC of different configurations in the three demand cases

Fig. 5(a) shows that in the $\frac{G}{D}$ = 1.62, the geothermal + HT-ATES can provide >99% of the heat, with geothermal energy alone already covering 84% of the heat demand. The gas boiler only contributes 0.4%. For the $\frac{G}{D}$ = 1.07 case, the RES remains high (94% for GGA), but it is lower than the $\frac{G}{D}$ = 1.62 case. The HT-ATES for this $\frac{G}{D}$ = 1.07 case increases the RES by 18 percentage points. For the $\frac{G}{D}$ = 0.65 case, the percentage directly provided by geothermal energy is 50%, with HT-ATES increasing this by 8 percentage points, which represents less actual heat provided by the HT-ATES than the $\frac{G}{D}$ = 1.07 case but more than the $\frac{G}{D}$ = 1.62 case. In terms of CO_2 savings, the GGA configuration saves about 10^4 tonne CO_2 per year in the $\frac{G}{D}$ = 1.07 and 0.65 cases compared to gas-only, while in the $\frac{G}{D}$ = 1.62 case, the savings are 6×10^3 tonnes CO_2 per year.

The CAC of geothermal is negative in all cases as it lowers the system LCOH (Fig. 5(b)). The CAC is more negative when a larger proportion of heat is supplied directly by geothermal energy. The most favourable CAC for geothermal is −0.35 €/kg CO_2, which occurs when all the heat of the geothermal doublet is directly supplied to the heat demand. This value is similar to the $\frac{G}{D}$ = 0.65 case. The HT-ATES has a positive CAC for the $\frac{G}{D}$ = 1.62 and 0.65 cases, while it is negative for the $\frac{G}{D}$ = 1.07 case. This indicates that while HT-ATES increases the RES in the $\frac{G}{D}$ = 1.62 and 0.65 cases, it also raises the system LCOH. The CAC is lowest in the $\frac{G}{D}$ = 1.07 case due to the favourable balance between stored and supplied heat.

5.3. Results parameter exploration

5.3.1. Geothermal capacity

The impact of geothermal capacity on the system LCOH and RES was explored (Fig. 6). Changes in system LCOH with varying geothermal capacity are shown in Fig. 6(a). Note, that by changing the geothermal capacity the $\frac{G}{D}$ value changes, while the scenario names remain the same, i.e., referring to the $\frac{G}{D}$ of the base scenario. For the GG configuration, the $\frac{G}{D}$ value with the lowest LCOH lies between 1.4 and 1.6. In the GGA configuration, the $\frac{G}{D}$ with the lowest LCOH range shifts to 1.1 to 1.3, with the minimum system LCOH being comparable to the GG configuration. Beyond that range, the system LCOH increases more sharply compared to the GG configurations, leading to a small range where the system LCOH is smaller than 90 €/MWh. This is due to higher operational costs for the HT-ATES, as well as larger CapEx of the geothermal doublet with diminishing return on investment. This aligns with previous findings that the $\frac{G}{D}$ = 1.07 case is the most cost-effective for the GGA configuration. This result shows the importance of considering the interplay between the heat supply, heat demand, and HT-ATES.

Examining the RES for three cases (Fig. 6(b)) reveals that achieving 100% RES is most cost-effective when combining geothermal heat with HT-ATES. However, the final few percentage points of RES are very cost-inefficient. For $\frac{G}{D}$ = 1.07 demand case, the LCOH of the GGA configuration rises from 81 to 85 and then to 104 €/MWh when increasing the RES target from 95% to 99% and 100%, respectively. A similar trend is observed for the other demand cases. This demonstrates that pushing the renewable energy share beyond 95% is cost-inefficient, with the last 1% causing a particularly sharp cost increase. Achieving this last 1% requires a large capacity for minimal load, driving costs up. Alternative strategies for this last 1% are discussed in Section 6. For the GG configuration, the increase in LCOH is even steeper at higher RES levels. However, below 80% RES, it is more cost-optimal to rely solely on the geothermal doublet.

5.3.2. HT-ATES maximum pumping rate

The results can be found in Fig. 7. The HT-ATES LCOH lines are not smooth due to the machine learning algorithm used in the HT-ATES model to predict the HT-ATES efficiency. This machine learning is shown to be more accurate at higher efficiency values [18]. With low pumping rates, the yearly injected volume decreases, which in turn leads to lower efficiency values compared to larger yearly injected volumes [33], in turn decreasing the accuracy of the HT-ATES model. This leads to some inconsistent results at low pumping rates.

For the $\frac{G}{D}$ = 1.62 demand case, the optimal HT-ATES LCOH occurs at a relatively low maximum pumping rate. Conversely, for the $\frac{G}{D}$ = 1.07 and 0.65 demand cases, the minimum HT-ATES LCOH is observed between a maximum pumping rate of 100 and 200 m^3/h. However, lower pumping rates in these cases slightly increase the system LCOH, as it forces more reliance on the gas boiler, which has a higher LCOH. Therefore, from the system perspective, a larger maximum pumping rate reduces the system LCOH. However, this effect is minimal, and the system LCOH is largely unaffected by the HT-ATES maximum pumping rate, due to HT-ATES only delivering a relatively small percentage of heat compared to the geothermal doublet (see Fig. 5(a)). Conversely, for the $\frac{G}{D}$ = 1.62 demand case, the system LCOH significantly increases

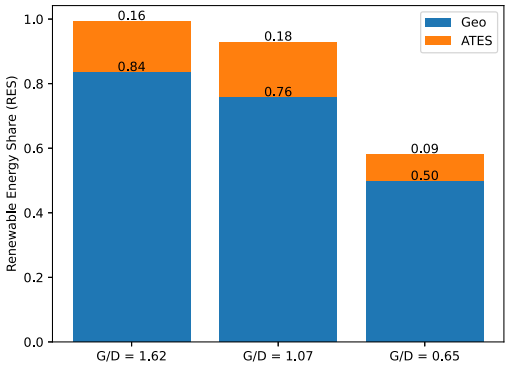

(a) RES of the two configurations and three demand cases. The gas boiler meets the remaining energy share.

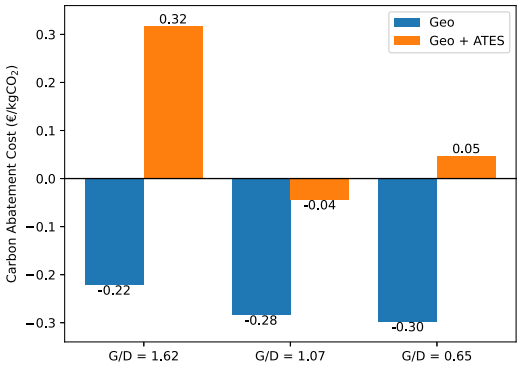

(b) CAC of the two configurations and three demand cases. Gas-only is left out as it has no reference case. The reference case for geothermal is the gas-only system, and for HT-ATES, the reference is the GG configuration.

Fig. 5. RES and CAC of the two configurations and three demand cases.

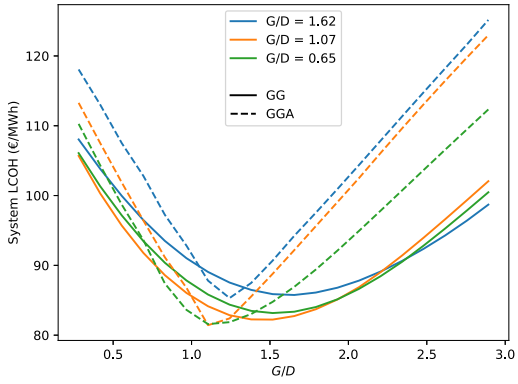

(a) System LCOH for different $\frac{G}{D}$ ratios, for the three demand cases and two configurations.

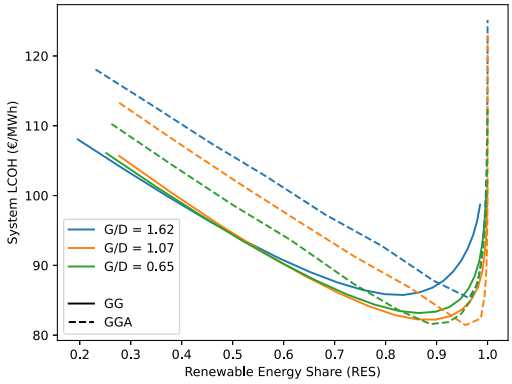

(b) System LCOH against the RES share of the system, obtained by varying the geothermal capacity and consequently, the $\frac{G}{D}$, for three demand cases and two configurations.

Fig. 6. LCOH and RES obtained by varying the geothermal capacity, the line colours correspond with the demands shown in Fig. 2.

with increasing maximum pumping rate. Lower maximum pumping rates would be beneficial.

HT-ATES increases the RES in all cases. The $\frac{G}{D} = 1.62$ case shows continued RES improvement with higher pumping rates, as HT-ATES can meet the entire remaining heat demand after geothermal supply, given a sufficiently high pumping rate (see Fig. 3(a)). This condition is not met in the other demand cases, where the heat demand exceeds what HT-ATES can provide, even at the highest pumping rates, and the RES lines flatten with increasing pumping rate.

5.3.3. Cut-off temperature

The impact of the cut-off temperature was analysed. As can be observed in Fig. 8, the impact of the cut-off temperature is twofold. First, it changes the capacity of the geothermal doublet due to variations in ΔT (as shown in Eq. (1)). Second, it influences the energy that can be delivered by the HT-ATES, as this is also dependent on ΔT. This effect is most apparent with the $\frac{G}{D} = 0.65$ case (Fig. 8(c)). At lower cut-off temperatures, both the geothermal doublet and HT-ATES produce significantly more heat than in the baseline, resulting in a notably low system LCOH. However, at higher cut-off temperatures, the geothermal doublet produces less heat and stores less in the HT-ATES, leading to less effective energy retrieval and a lower RES.

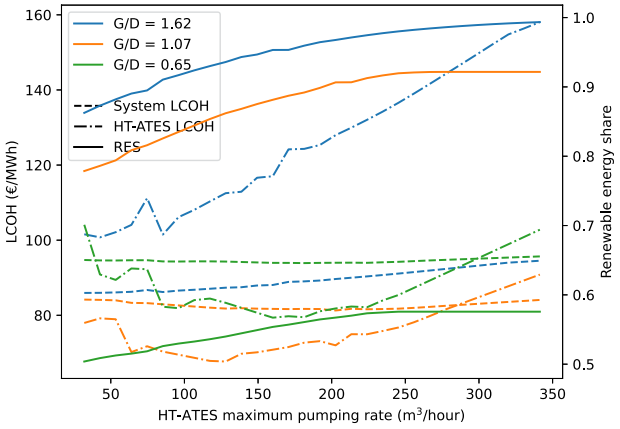

Fig. 7. LCOH of the HT-ATES, LCOH of the system, and RES for three cases with the GGA configuration.

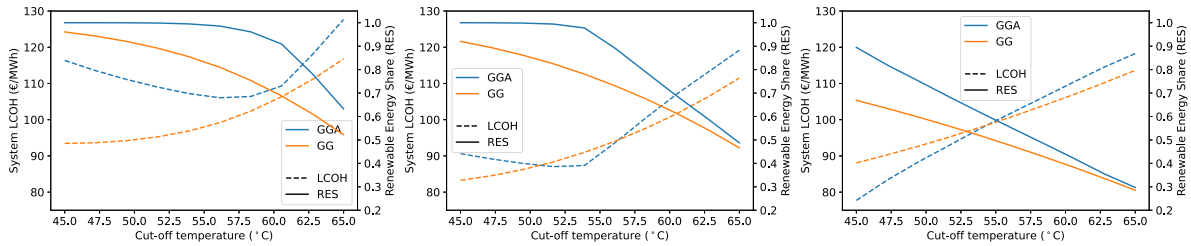

(a) LCOH and RES for $\frac{G}{D}$ = 1.62 case (b) LCOH and RES for $\frac{G}{D}$ = 1.07 case (c) LCOH and RES for $\frac{G}{D}$ = 0.65 case

Fig. 8. The impact of the cut-off temperature on RES and system LCOH for the different demand cases.

Table 3
LCOH of the different calculation methods of the HT-ATES component.

	LCOH Reduced efficiency	LCOH Constant efficiency	Difference
$\frac{G}{D}$ = 1.62	119 €/MWh	115 €/MWh	4 €/MWh
$\frac{G}{D}$ = 1.07	72 €/MWh	70 €/MWh	2€/MWh
$\frac{G}{D}$ = 0.65	83 €/MWh	80 €/MWh	3 €/MWh

In both the $\frac{G}{D}$ = 1.62 and 1.07 cases, the LCOH line of the GGA is shown to have an optimum that is not at the lowest possible cut-off temperature. This is due to the RES values reaching 99%, and any further decrease in cut-off temperature only leads to an increase of system LCOH due to increased operational cost for storing heat in the HT-ATES system without increased energy delivered (Fig. 8(a)). This is because of the control system. The control system ensures that all excess energy is stored. While if not all of the excess energy can be used, it is more economically beneficial to also store less heat in the HT-ATES. This aspect could be explored further in future studies.

5.3.4. Constant HT-ATES recovery efficiency

One of the research assumptions in this study is that the recovery efficiency of the HT-ATES is lower during the first few years of operation. It is incorporated in the applied HT-ATES model. If this is not taken into account during calculations, the LCOH will be lower. The impact of this assumption on the HT-ATES LCOH is examined. The results are shown in Table 3. As can be seen with a reduced efficiency, the LCOH increases by a small percentage (around 3%) compared to the constant efficiency. This is because the HT-ATES delivers less energy during the first few years, reducing E_i in Eq. (2), thereby increasing the LCOH, compared to the constant efficiency. However, the effect of this difference is small.

5.3.5. Peak shaving

One example of the demand curve where peak shaving is applied is shown in Fig. 9. The only difference between this figure and Fig. 3(b) is when the heat of the HT-ATES is used. This peak shaving only leads to a lower required backup capacity, in this case, a gas boiler. However, the reduction in gas boiler LCOH is 0.0 €/MWh, 0.8 €/MWh, and 1.3 €/MWh for the cases $\frac{G}{D}$ = 1.62, 1.07, and 0.65, respectively. And for all three cases, the reduction in system LCOH is less than 0.1 €/MWh. It is most economically beneficial to apply peak shaving with the $\frac{G}{D}$ = 0.65 case. As pointed out before, for both the $\frac{G}{D}$ = 1.62 and 1.07 case there is very little heat that is covered by the gas boiler (see Fig. 5(a)), therefore, there is no flexibility in the operation of the HT-ATES, while for $\frac{G}{D}$ = 0.65, the amount of heat stored in the HT-ATES is significant, and peak shaving is useful for reducing backup capacity.

The economic impact of peak shaving is small. However, if other considerations constrain the gas boiler capacity, the HT-ATES can provide peak shaving and, therefore, reduce the needed gas boiler capacity.

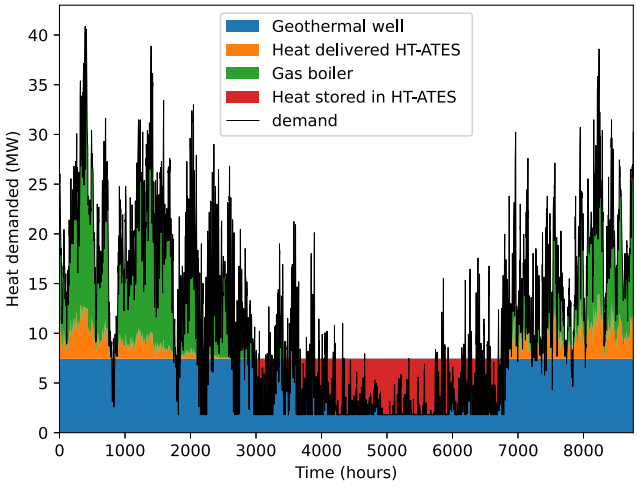

Fig. 9. Using the HT-ATES as peak shaving unit for the $\frac{G}{D}$ = 0.65 case.

5.4. Monte Carlo LCOH distribution and sensitivity analysis

Fig. 10 presents the system LCOH distribution resulting from the Monte Carlo analysis. The $\frac{G}{D}$ = 1.07 case has the lowest system LCOH of the three cases. The P90 value for $\frac{G}{D}$ = 1.07 is lower than the P10 case of $\frac{G}{D}$ = 0.65 and 1.62. The $\frac{G}{D}$ = 1.07 system LCOH distribution differs significantly from the other two. While $\frac{G}{D}$ = 0.65 and 1.62 largely overlap.

The distribution is highly dependent on the different parameters (Fig. 11). For both $\frac{G}{D}$ = 1.62 and 1.07, the CapEx of the geothermal doublet is the most influential factor. This is attributed to the geothermal doublet's significant share in total heat supply, its high investment costs, and the variability in these costs assigned during the Monte Carlo analysis (Figs. 11(a) and 11(b)). For $\frac{G}{D}$ = 1.62, both the gas price and the CapEx of the geothermal doublet are important factors. This is due to a large share of heat being provided by the gas boiler, and the variability in gas price affects the system LCOH more significantly.

6. Discussion

In this study, a methodology was developed to simulate the DH system and its individual components, enabling the calculation of key

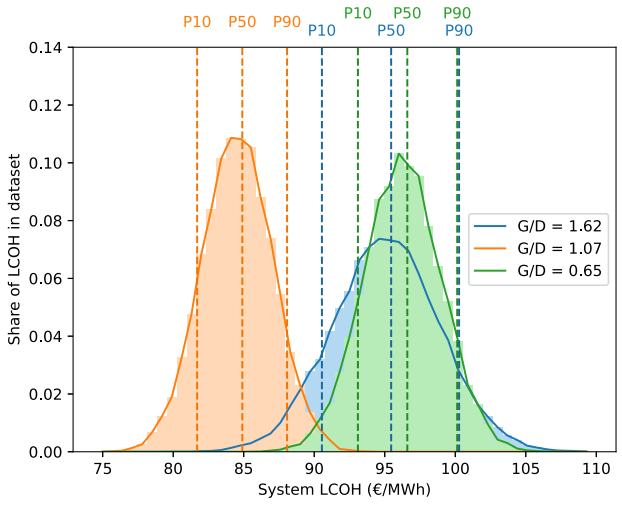

Fig. 10. The distribution of system LCOH of the three demand cases for the GGA configuration, resulting from the Monte Carlo analysis with 20,000 iterations. P10 lines define the lowest 10% of the data, P50 defines the lowest 50%, and P90 defines the lowest 90%. The ranges of LCOH between the P10 and P90 lines are 91–100, 82–88, and 93–100 €/MWh for $\frac{G}{D}$ = 1.07, 0.65, and 1.62, respectively.

performance indicators such as the LCOH, RES, and CAC across various DH configurations. This approach was applied to assess and examine a case study. Additionally, a sensitivity analysis was performed to assess the effect of different important parameters.

The case study showed that integrating geothermal energy and HT-ATES can significantly reduce the use of gas boilers. Our case study also reveals that geothermal energy can significantly reduce both the system LCOH and increases the RES. It was found that the optimal sizing for a geothermal system was around a $\frac{G}{D}$ of 1.5. For HT-ATES, the cost reduction depends on the relation between supply and demand, and an optimal $\frac{G}{D}$ around 1.2 was found. Practically, the geothermal doublet is usually installed first, which presents a sizing challenge, as the geothermal doublet can be sized to be economically optimal without the HT-ATES at $\frac{G}{D}$ was shown to be 1.5. However, that also restricts the use of HT-ATES, as the system LCOH of GGA with a large geothermal doublet (around $\frac{G}{D}$ of 1.5), is significantly larger. This should be considered when implementing renewable technologies.

For the case study, the $\frac{G}{D}$ = 0.65 case has limited excess heat available for storage, resulting in higher costs when utilizing a HT-ATES, while the $\frac{G}{D}$ = 1.62 case's minimal demand for stored heat leads to underutilization of the heat stored in the HT-ATES. Therefore, careful planning of the system configuration design is required to match HT-ATES capacities with demand profiles and sustainable heat supply capacity to ensure cost-effectiveness. However, in all scenarios the use of HT-ATES was shown to increase the renewable energy share by 9 to 18%.

This study underscores the need to evaluate the economic and environmental performance of HT-ATES within the broader context of a heating system. The scale of heat demand and the capacity of the available heat source both affect the operation and efficiency of the HT-ATES. Consequently, future analyses of HT-ATES performance should explicitly account for the interactions between the HT-ATES, the heat supplier, and the heat demand.

From an economic perspective, in the conceptual case study examined, the HT-ATES is economically beneficial in some cases, but in other cases, it increases the system LCOH. The specific conclusions here must be viewed in the context of the example numbers included for the costs of gas, the geothermal system and the HT-ATES. The HT-ATES increases the RES with a CAC ranging from −0.04 to 0.32 €/kgCO_2. In comparison, heat pumps have a CAC, recorded in the literature, between −0.01 and −0.04 €/kgCO_2 and solar thermal has a CAC between −0.01 and 0.05 €/kgCO_2 [20]; HT-ATES can compete with these technologies when applied to the $\frac{G}{D}$ = 1.07 or $\frac{G}{D}$ = 0.65 demand case, mainly because in these cases, there is both sufficient excess heat and unmet demand. For both cases, the avoided CO_2 compared to only using gas boilers is similar (10^4 tonne CO_2 on a yearly basis). Additionally, the HT-ATES abates the peaks of demand. These peaks are significantly more expensive to abate because they occur infrequently, and increasing the capacity of alternative technologies solely to meet peak demand is also costly. When sufficient excess heat and unmet demand are both present, the HT-ATES can achieve a CAC comparable to that of other technologies, while simultaneously supplying peak demand. This capability is particularly valuable when fully transitioning to renewable heat.

As shown in the $\frac{G}{D}$ = 1.62 case, a RES of >99% is, however, not cost-effective because the system LCOH is high. It is caused by the high investment cost for the HT-ATES while only providing a small share of energy. This indicates that aiming for 100% RES targets from a financial standpoint can be significantly less attractive than targeting a slightly lower RES target (around 95% RES), and less effective when the investment can be used in another system. Specifically, in this case, the last 1% of the RES was shown to be cost-inefficient to achieve. Other solutions might be considered for this last 1%. An example would be peak shaving via methods other than using the HT-ATES. This would reduce the peaks that are the hardest to abate. This could be done via demand management on the DH operator side, which moves the demand from these peak hours to lower demand hours using daily buffers [38]. Another approach is to reduce peaks by changing the building occupants' heating behaviour. Lowering the targeted indoor temperature is an example.

Furthermore, these numerical results are obtained from a case study, but the proposed methods are applicable to other cases. Examples include DH systems in different climate zones and DH systems in horticulture sectors, e.g., greenhouses [39].

The dynamic interplay between systems is shown to be highly non-linear. This work can inform project developers about how to design their system to achieve their aims, however as governments regularly apply subsidy schemes with the objective of stimulating certain objectives (e.g. avoiding CO_2 emissions), this work can also be used to aid the design of the most cost-effective schemes to achieve their aims.

This study has some limitations. First, it assumes fixed supply and return temperatures, whereas in reality, they fluctuate with outdoor temperature and heat demand, often requiring higher temperatures during peak demand [15]. Future work should incorporate temperature-dependent supply and return profiles and investigate how dynamic operating temperatures affect HT-ATES charging strategies, storage efficiency, and overall system economics. Secondly, heat pumps are not incorporated in this study, which could have been coupled to either the geothermal doublet or the HT-ATES to boost the temperature (as in [14]). Future studies should investigate the feasibility of coupling a heat pump to an HT-ATES and examine the costs and benefits. Thirdly, ramp-up and ramp-down times of heat suppliers were not considered, which might constrain the heat supply. However, time steps of one hour are used, which are often large enough to neglect these effects. Additionally, CapEx of both the geothermal doublet and HT-ATES is a linear function of capacity. In reality, this is more nuanced and related to the depth of the systems and technologies used. This was avoided to enable a fair comparison between different $\frac{G}{D}$ scenarios, but future studies could investigate how the cost and subsurface properties are related. Lastly, future changes such as increased insulation are not taken into account and can play a major role in demand reduction, which in turn impacts the economics of the HT-ATES.

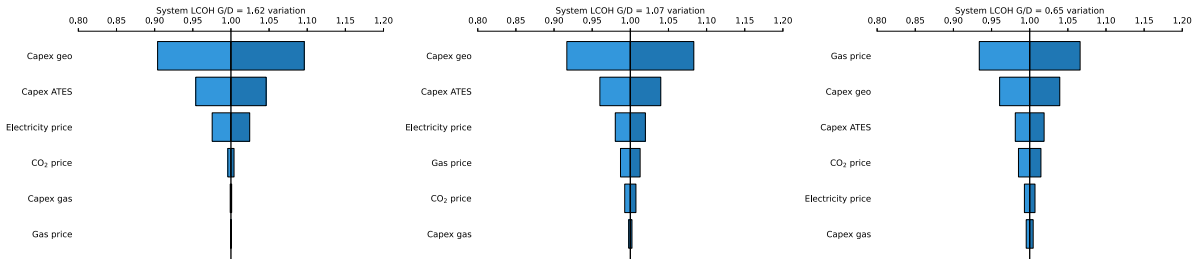

(a) $\frac{G}{D}$ = 1.62 (b) $\frac{G}{D}$ = 1.07 (c) $\frac{G}{D}$ = 0.65

Fig. 11. Key drivers of variance in system LCOH. Calculated LCOH at 2 times the standard deviation from the mean of each parameter while keeping every other parameter at their mean value. LCOH of 1 refers to the LCOH calculated at mean values.

7. Conclusion

This study presents a methodology for techno-economic and environmental assessment of a sustainable District Heating (DH) system with a High-Temperature Aquifer Thermal Energy Storage (HT-ATES). The main contribution of the methodology is to include the dynamics of the interplay between the different components. The methods were applied to a case study, a simplified DH system conceptually based on a system being implemented in Delft, the Netherlands. This work emphasizes the importance of understanding the impact of the interaction between heat demand, heat supply technologies, and storage technologies on economic performance. Key metrics such as the Levelized Cost Of Heat (LCOH), Renewable Energy Share (RES), and Carbon Abatement Cost (CAC) were evaluated, and the sensitivity of these metrics to various important parameters was demonstrated.

We show that for the case study, a geothermal project alone reduces the system LCOH by 27%, 30%, and 21% with a ratio of Geothermal to Demand ($\frac{G}{D}$) = 1.62, 1.07, and 0.65, respectively. Adding an HT-ATES only decreases the system LCOH in the $\frac{G}{D}$ 1.07 case and does so by 1.5%, while also increasing RES by the largest amount. This indicates that the relationship between the heat demand and supply technologies is vital for the effectiveness of implementing HT-ATES. The HT-ATES is more efficient when large amounts of excess heat are stored. However, if the amount of heat stored significantly exceeds the demand, HT-ATES becomes underutilized, negatively impacting economic performance, which in this research led to a LCOH of HT-ATES 157 €/MWh, where the lowest HT-ATES LCOH is 86 €/MWh. Achieving a balance between heat storage and extraction is thus crucial for maximizing both economic viability and efficiency of the HT-ATES. Ignoring these aspects leads to an incomplete assessment of the HT-ATES.

We showed that once RES approaches 100%, LCOH rises due to higher operational costs and overcapacity, making 100% RES economically inefficient, with mostly the last 1% being very cost-ineffective. However, a geothermal + HT-ATES combination remains the most cost-effective way to achieve 100% RES in the case examined.

The geothermal doublet was shown to have a negative CAC and is economically beneficial while also reducing CO_2 emissions compared to a gas-only system. For HT-ATES, the CAC is highly dependent on the balance between heat storage and extraction. Insufficient stored or extracted heat results in a positive CAC, where CO_2 emissions are reduced, but it increases the system LCOH. The CAC of the HT-ATES can be negative under the right circumstances, which highlights the importance of including the interplay between DH components in the analysis, by matching storage capacity to demand patterns to ensure economic viability.

Finally, the sensitivity analysis showed that the lowest system LCOH could be found for a $\frac{G}{D}$ around 1.5 when only using geothermal and for geothermal + HT-ATES, the optimal $\frac{G}{D}$ = around 1.2, indicating that over-sizing the geothermal doublet relative to the total demand is economically beneficial. This also indicates that when installing a geothermal project, an early decision has to be made whether to also include HT-ATES, as the optimal sizing of geothermal differs with and without the HT-ATES.

CRediT authorship contribution statement

David Geerts: Writing – original draft, Visualization, Software, Methodology, Investigation, Data curation, Conceptualization. **Wen Liu:** Writing – review & editing, Visualization, Supervision, Methodology, Funding acquisition. **Alexandros Daniilidis:** Writing – review & editing, Supervision, Funding acquisition. **Philip J. Vardon:** Writing – review & editing, Funding acquisition, Conceptualization. **Gert Jan Kramer:** Writing – review & editing.

Declaration of competing interest

The authors declare that they have no known competing financial interests or personal relationships that could have appeared to influence the work reported in this paper.

Acknowledgements

This work was funded by the European Union under the Horizon Europe programme (grant no. 1011096566). Views and opinions expressed are however those of the author(s) only and do not necessarily reflect those of the European Union or CINEA. Neither the European Union nor CINEA can be held responsible for them.

Data availability

Data will be made available on request.

References

[1] IEA. Space heating. Tech. Rep., IEA; 2023, [Online]. Available: https://www.iea.org/reports/space-heating.
[2] Cozzi L, Gould T, Bouckart S, Crow D, Kim T, Mcglade C, Olejarnik P, Wanner B, Wetzel D. World energy outlook 2020. vol. 2050, Paris, France: IEA; 2020, p. 1–461.
[3] Werner S. International review of district heating and cooling. Energy 2017;137:617–31.
[4] Irena. Geothermal power; Technology brief. Tech. Rep., Irena; 2017.
[5] Sanchez-Lorenzo A, Calbó J, Martin-Vide J. Spatial and temporal trends in sunshine duration over western Europe (1938–2004). J Clim 2008;21(22):6089–98.
[6] Bloemendal M, Hartog N. Analysis of the impact of storage conditions on the thermal recovery efficiency of low-temperature ATES systems. Geothermics 2018;71:306–19.
[7] Yang T, Liu W, Kramer GJ, Sun Q. Seasonal thermal energy storage: A techno-economic literature review. Renew Sustain Energy Rev 2021;139:110732.
[8] Vanhoudt D, Desmedt J, Van Bael J, Robeyn N, Hoes H. An aquifer thermal storage system in a belgian hospital: Long-term experimental evaluation of energy and cost savings. Energy Build 2011;43(12):3657–65.
[9] Schmidt T, Müller-Steinhagen H. The central solar heating plant with aquifer thermal energy store in rostock-results after four years of operation. In: Proceedings of eurosun. 2004.
[10] Kabus F, Wolfgramm M, Seibt A, Richlak U, Beuster H. Aquifer thermal energy storage in neubrandenburg-monitoring throughout three years of regular operation. In: Proceedings, EFFSTOCK conference, Stockholm. 2009, p. 1–8.

[11] Narula K, De Oliveira Filho F, Chambers J, Romano E, Hollmuller P, Patel MK. Assessment of techno-economic feasibility of centralised seasonal thermal energy storage for decarbonising the swiss residential heating sector. Renew Energy 2020;161:1209–25.
[12] Dobson P, McLing T, Spycher N, Fleuchaus P, Neupane G, Doughty C, Zhang Y, Smith R, Atkinson T, Jin W, et al. High-temperature aquifer thermal energy storage (HT-ATES) projects in Germany and the Netherlands—Review and lessons learned. Energies (19961073) 2025;18(23).
[13] Guglielmetti L, Lehu R, Daniilidis A, Valley B, Moscariello A. Spatial multi-criteria play-based analysis for HT-ATES systems across the swiss molasse plateau. Energy Rep 2025;14:85–102.
[14] Daniilidis A, Mindel JE, De Oliveira Filho F, Guglielmetti L. Techno-economic assessment and operational CO2 emissions of high-temperature aquifer thermal energy storage (HT-ATES) using demand-driven and subsurface-constrained dimensioning. Energy 2022;249:123682.
[15] Bloemendal M, Vardon P, Medema A, Snelleman S, Marif K, Beernink S, van Veldhuizen F, Pijnenborg M, Sudintas G, van Oort T. HT-ATES at the TU Delft campus. Tech. Rep., 2020, [Online]. Available: https://www.warmingup.info/documenten/window-fase-1—a1—verkenning-hto-tud—feasibilityht_ates_tudelft.pdf.
[16] Remmelts J, Tensen S, Ferreira CI. Seasonal thermal energy storage for large scale district heating. In: 13th IEA heat pump conference; 26.-29.04. 2021; Jeju, Korea. Borås, Sweden. Heat Pump Centre c/o RISE Research Institutes of Sweden; 2021, p. 1633–43.
[17] Bolton R, Cameron L, Kerr N, Winskel M, Desguers T. Seasonal thermal energy storage as a complementary technology: Case study insights from Denmark and The Netherlands. J Energy Storage 2023;73:109249.
[18] Geerts D, Daniilidis A, Liu W. A fast and accurate data-driven model for estimating the production temperature of high-temperature aquifer thermal energy storage. Appl Therm Eng 2025;126817.
[19] Vakkilainen EK. Steam generation from biomass: Construction and design of large boilers. Butterworth-Heinemann; 2016.
[20] IEA. Sustainable recovery. Tech. Rep, IEA; 2020, [Online]. Available: https://iea.blob.core.windows.net/assets/c3de5e13-26e8-4e52-8a67-b97aba17f0a2/Sustainable_Recovery.pdf.
[21] van't Westende J, Dinkelman D. Feasibility study for combined geothermal and HT-ATES systems. Tech. Rep., 2023, [Online]. Available: https://www.warmingup.info/documenten/feasibility-study-for-combined-geothermal-and-ht-ates-systems.pdf.
[22] Koelemeijer R, van Hout M, Ooms E, van Dam D, Koole G. Analyse tarief CO2-heffing industrie. Tech. Rep., PBL; 2024.
[23] Lensink S, Eggink E, Schoots K. Eindadvies basisbedragen sde++ 202. Tech. Rep., PBL; 2022.
[24] van de Griendt T. Benefits of high-temperature storage for base load geothermal energy. 2022.
[25] European energy exchange. 2024, https://www.eex.com/en/market-data/natural-gas/indices. [Accessed 25 June 2024].
[26] Wright ML, Lewis AC. Emissions of NO x from blending of hydrogen and natural gas in space heating boilers. Elementa Sci Anthropocene 2021;10(1):00114.
[27] Zeilema P. The Netherlands: List of fuels and standard CO2 emission factors version of January 2022. 2022, [Online]. Available: https://www.rvo.nl/sites/default/files/2023-08/The%20Netherlands%20list%20of%20fuels%20and%20standard%20CO2%20emission%20factors%20January%202022.pdf.
[28] Eurostat. Electricity price statistic. 2024, https://ec.europa.eu/eurostat/statistics-explained/index.php?title=Electricity_price_statistics#Electricity_prices_for_non-household_consumers. [Accessed 25 June 2024].
[29] Fleuchaus P. Global application, performance and risk analysis of aquifer thermal energy storage (ATES) [Ph.D. dissertation], Karlsruher Institut für Technologie (KIT); 2020.
[30] Naber N, Dehens J. Update kentallen installaties Vesta MAIS. Tech. Rep., CE Delft; 2022, [Online]. Available: https://ce.nl/wp-content/uploads/2023/03/CE_Delft_210348_Update_kentallen_installaties_Vesta_MAIS_Def.pdf.
[31] Herreras Martínez S, Uyttewaal M, Liu W, Harmsen R. Exploring sustainable heating solutions for buildings at the neighbourhood level. Energy Effic 2021;14(8):93.
[32] Kim J, Weidlich I. Identification of individual district heating network conditions using equivalent full load cycles. Energy Procedia 2017;116:343–50.
[33] Geerts D, Daniilidis A, Kramer GJ, Bloemendal M, Liu W. Analytically estimating the efficiency of high temperature aquifer thermal energy storage. Geotherm Energy 2025;13(1):17.
[34] Sheldon HA, Wilkins A, Green CP. Recovery efficiency in high-temperature aquifer thermal energy storage systems. Geothermics 2021;96:102173.
[35] EU natural gas TTF. 2025, https://tradingeconomics.com/commodity/eu-natural-gas. [Accessed 24 February 2025].
[36] Prices of natural gas and electricity. 2025, https://www.cbs.nl/en-gb/figures/detail/85666ENG. [Accessed 24 February 2025].
[37] Maximumtarieven warmte in 2025: Variabel tarief omlaag, vaste kosten bijna gelijk. 2025, https://www.acm.nl/nl/publicaties/maximumtarieven-warmte-2025-variabel-tarief-omlaag-vaste-kosten-bijna-gelijk. [Accessed 24 January 2025].
[38] Arnaudo M, Topel M, Puerto P, Widl E, Laumert B. Heat demand peak shaving in urban integrated energy systems by demand side management-a techno-economic and environmental approach. Energy 2019;186:115887.
[39] Geerts D, Daniilidis A, Kramer GJ, Liu W. Sizing optimization of district heating components with high-temperature aquifer thermal energy storage: Techno-economic analysis. 2025, Under review.